

Invisible Watermarks, Visible Gains: Steering Machine Unlearning with Bi-Level Watermarking Design

Yuhao Sun^{1,2*}, Yihua Zhang³, Gaowen Liu⁴, Hongtao Xie¹, Sijia Liu³

¹University of Science and Technology of China,

²Institute of Artificial Intelligence, Hefei Comprehensive National Science Center,

³Michigan State University, ⁴Cisco Research

Abstract

With the increasing demand for the right to be forgotten, machine unlearning (MU) has emerged as a vital tool for enhancing trust and regulatory compliance by enabling the removal of sensitive data influences from machine learning (ML) models. However, most MU algorithms primarily rely on in-training methods to adjust model weights, with limited exploration of the benefits that data-level adjustments could bring to the unlearning process. To address this gap, we propose a novel approach that leverages digital watermarking to facilitate MU. By integrating watermarking, we establish a controlled unlearning mechanism that enables precise removal of specified data while maintaining model utility for unrelated tasks. We first examine the impact of watermarked data on MU, finding that MU effectively generalizes to watermarked data. Building on this, we introduce an unlearning-friendly watermarking framework, termed WATER4MU, to enhance unlearning effectiveness. The core of WATER4MU is a bi-level optimization (BLO) framework: at the upper level, the watermarking network is optimized to minimize unlearning difficulty, while at the lower level, the model itself is trained independently of watermarking. Experimental results demonstrate that WATER4MU is effective in MU across both image classification and image generation tasks. Notably, it outperforms existing methods in challenging MU scenarios, known as “challenging forgets”.

1. Introduction

Machine unlearning (MU), which aims to remove the influence of unwanted data from a pre-trained model while preserving the model’s utility on data unrelated to the unlearning request, has emerged as a promising approach for customizing and adapting machine learning (ML) models

*This work was conducted during a remote research visit to the OPTML Group at Michigan State University.

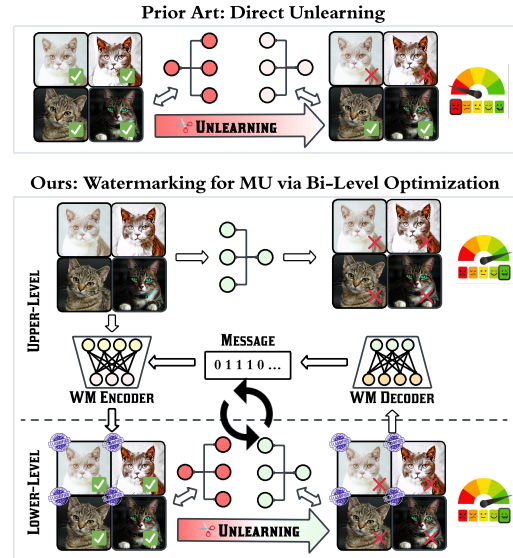


Figure 1. An overview of the watermarking for machine unlearning framework via bi-level optimization proposed in this work.

to diverse contexts and requirements [1–4]. For example, MU is widely used to enhance model privacy, aligning with the right to be forgotten by removing private or copyrighted information from models to prevent privacy breaches [5–9]. It has also been applied to improve model generalization in transfer learning by removing the influence of undesired source data in pre-trained models, where removing non-salient source data to downstream tasks improves fine-tuning performance [10, 11]. Furthermore, MU shows promise in enhancing model robustness, for instance, by removing the influence of backdoored training data to defend against backdoor attacks [12, 13] or eliminating harmful data to improve the model’s trust [14–16].

The expanding applications of MU across diverse domains and model types—including discriminative and generative models [17, 18]—are driven by its effectiveness in erasing specific data influence within ML models. That is, a key aspect of MU involves characterizing the influence of specific data on the model and leveraging this data-model

interaction to adjust the model for effective unlearning. However, predominant research in MU focuses on model-based weight updating as the primary approach to achieve the unlearning objective [19–25], with less attention given to the impact of data modifications—such as *watermarking*, which we will investigate in this work—on MU effectiveness.

Digital watermarking, which embeds ownership signatures (known as watermark messages) into digital content such as images, serves as a valuable tool for tracking data origin and deterring unauthorized use or distribution [26–28]. Despite the variety of watermarking techniques [29–33], they provide an effective means to *proactively* modify data points in ways that are imperceptible to human users. Deep learning-based watermarking techniques [31, 34], in particular, offer automated methods to embed and extract watermark messages from watermarked data. If we consider watermarking as a (privacy-preserving) data modification operation, intriguing questions arise on how it influences unlearning process and whether it can be strategically controlled to facilitate unlearning. Thus, we ask:

(Q) What is the impact of watermarking on unlearning, and how can it be guided to facilitate unlearning?

To address (Q), we focus on watermarking for imagery data and MU in the context of image classification. We consider two paradigms for integrating MU with watermarking. First, in the paradigm of MU for watermarking, we investigate the generalization of the exact unlearning approach, where the image classifier is retrained from scratch with the data samples to be forgotten excluded. We examine how this approach generalizes to watermarked training samples (used in the unlearning optimization process) and watermarked testing samples (used in unlearning evaluation). We find that unlearning generalizes well to watermarked data; watermarking appears to be orthogonal to unlearning and has minimal negative impact on its effectiveness. Inspired by this, we consider the second paradigm of watermarking for MU, where we investigate whether the watermarking design can be customized to favor MU. This allows us to proactively watermark data in a way that facilitates the unlearning optimization process. The proposed MU-aware watermarking method is referred to as WATER4MU. We provide a schematic overview of WATER4MU in Fig. 1. In what follows, we summarize **our contributions**.

- To the best of our knowledge, this is the first work to investigate the influence of watermarking on MU and to explore their interactions.
- We develop WATER4MU using bi-level optimization, enabling the watermarking mechanism to enhance MU by designing the watermarking network and selecting watermark messages to support unlearning when requested.
- We validate the advantages of incorporating watermarking into MU for image classification and generation by com-

paring the performance of WATER4MU with existing MU methods in their standard forms.

2. Related Work

Machine unlearning (MU). MU focuses on modifying ML models to remove the influence of specific data points, classes, or broader knowledge-level concepts [6, 35–38]. A widely-recognized exact unlearning approach, termed Retrain, involves retraining the model from scratch after omitting the data points to be forgotten [22, 39]. While Retrain provides the ideal removal of data influences [40, 41], its computational cost and lack of scalability render it impractical for large-scale deep learning models. To address these limitations, numerous studies have proposed approximate unlearning methods that aim to achieve efficient unlearning without requiring full model retraining [11, 19, 20, 22, 23, 25, 35–38, 42].

MU for image classification has predominantly centered on two scenarios: (random) data-wise forgetting and class-wise forgetting. The former involves eliminating the influence of randomly chosen data points from the training set, while the latter aims to remove the effects of an entire image class. As MU research has evolved, its applications have also extended beyond image classification to encompass other domains. For example, MU has been applied to erasing specific concepts from diffusion models [9, 15, 25, 43–46]. Beyond vision tasks, MU is increasingly recognized for its potential to enhance the trustworthiness of data-model relationships in other fields, such as federated learning [47–49] and large language models (LLMs) [50–53].

Digital watermarking. Digital watermarking serves a wide range of purposes, including copyright protection, content authentication, and data provenance tracking [54–56]. It embeds hidden information, known as a watermark message, into digital images in a way that is imperceptible to human observers but can be extracted using specific algorithms. Traditional watermarking techniques have primarily focused on transform-domain methods, such as discrete cosine transform (DCT) [57, 58], discrete wavelet transform (DWT) [59], and singular value decomposition (SVD) [60], embedding watermarks within the frequency or singular value domains of images. Recent advances in ML have driven the development of deep learning-based watermarking techniques. One prominent example is HIDDEN [31], which uses an encoder-decoder framework to efficiently embed and extract watermarks from images. Expanding on this approach, methods like DeepStego [61] leverage adversarial learning to improve the visual fidelity of watermarked images while maintaining robust watermark extraction. Although prior studies have examined how watermarked data affects various visual tasks [62, 63], the relationship between digital watermarking and MU has remained largely unexplored. This work seeks to address this gap by investigating

how watermarking can be utilized to support and enhance MU processes, offering new insights into their interaction and potential synergies.

Visual prompting. Visual prompting (VP) was initially introduced by [64, 65] as an adaptation of prompting methods from natural language processing (NLP) to computer vision. A closely related concept, adversarial reprogramming or model reprogramming, was previously applied in computer vision to repurpose fixed pretrained models for new tasks [66–73]. Recent advancements have refined VP techniques by optimizing label mappings [70, 74] and introducing improved normalization methods [75]. The versatility of VP has also been demonstrated across various applications, including adversarial defense [76, 77], enhancing differential privacy [78], advancing model sparsification [79], improving model generalization [80, 81], and addressing distributional shifts [82, 83]. Furthermore, VP has been effectively extended to vision-language models, enabling better integration and adaptation for multimodal tasks [84–86].

3. Preliminaries and Problem Statement

MU setup and formulation. The *goal* of MU is to remove the influence of specific (undesired) training data from a pre-trained ML model while retaining its normal model utility. To formalize, let $\mathcal{D} = \{\mathbf{z}_i\}_{i=1}^N$ denote the training dataset with N data points, where each data point includes a feature vector \mathbf{x}_i and label y_i in a supervised learning setup. We define $\mathcal{D}_f \subseteq \mathcal{D}$ as the dataset subset we aim to forget, termed the *forget set*, and let $\mathcal{D}_r = \mathcal{D} \setminus \mathcal{D}_f$ denote the *retain set*, comprising the data to be preserved.

Retraining the model from scratch solely on the retain set \mathcal{D}_r is generally regarded as the gold standard in MU, as it minimizes privacy leakage of the forget data in \mathcal{D}_f post-retraining and is considered an *exact* unlearning approach [11, 22, 87]. However, retraining is computationally intensive and often impractical. Consequently, current research has focused on *approximate* unlearning methods [3, 20, 21, 23, 88], which aim to achieve efficient unlearning directly from an already-trained model, without the need for retraining from scratch. Let θ_o denote the original model trained on the full dataset \mathcal{D} using, for instance, empirical risk minimization. Approximate unlearning can be framed as a fine-tuning problem, as outlined below:

$$\begin{aligned} \theta_u &:= \arg \min_{\theta} \mathcal{L}_{\text{mu}}(\theta; \mathcal{D}_f, \mathcal{D}_r) \\ &:= \lambda_f \ell_f(\theta; \mathcal{D}_f) + \lambda_r \ell_r(\theta; \mathcal{D}_r), \end{aligned} \quad (1)$$

where θ_u represents the unlearned model (*i.e.*, the updated model after unlearning from the original model θ_o).

In (1), the terms ℓ_f and ℓ_r represent the forget and retain losses, respectively. The former characterizes the unlearning objective on the forget set, often defined as the *negative* of the cross-entropy (CE) based prediction loss (ℓ_{CE}) to effectively reverse the influence of the forget data. The latter,

analogous to standard ERM, enforces the preservation of the model’s utility on the retain set, ensuring that performance on unaffected data remains intact. There is generally a tradeoff between unlearning effectiveness (*i.e.*, minimizing ℓ_f) and preserving model utility (*i.e.*, minimizing ℓ_r). To balance this, regularization parameters $\lambda_f \geq 0$ and $\lambda_r \geq 0$ are introduced in (1) for controlled adjustment between these objectives. If we set $\lambda_f = 1$, $\lambda_r = 0$, and $\ell_f = -\ell_{\text{CE}}$, then solving the problem reduces to the classic gradient ascent (GA) approach for MU [22]. If we set $\lambda_f = 0$, $\lambda_r = 1$, and $\ell_r = \ell_{\text{CE}}$, then problem (1) reduces to the classic fine-tuning (FT) approach, which leverages catastrophic forgetting to achieve unlearning [20].

Image watermarking. Digital watermarking is another fundamental tool employed in this paper, which involves embedding hidden information (referred to as the “watermark message”) into original imagery data through a watermarking process. This then allows for the watermark message to be extracted through a decoding process. Such an encoding-decoding watermarking technique has been used to assert data ownership and authenticate content [26–28].

Formally, the watermarking problem can be defined as follows: Given an input image \mathbf{x} and an L -bit watermark message $\mathbf{m} \in \{0, 1\}^L$, the objective is to generate a watermarked image \mathbf{x}_w that preserves visual similarity to the original image \mathbf{x} while embedding the watermark message \mathbf{m} . Additionally, the watermarked image \mathbf{x}_w should be constructed to allow reverse engineering of its embedded message \mathbf{m} , thereby enabling the identification of the image’s origin. To this end, we adopt HIDDEN [31] as the watermarking method—a widely used deep neural network-based image watermarking framework. It comprises an encoder f_ψ and a decoder g_ϕ , with network parameters ψ and ϕ , respectively. The encoder f_ψ takes the original image \mathbf{x} and the message \mathbf{m} as input, producing the watermarked image $\mathbf{x}_w = f_\psi(\mathbf{x}, \mathbf{m})$. The decoder g_ϕ then aims to recover the watermark message from \mathbf{x}_w , yielding an extracted message denoted as $\hat{\mathbf{m}} = g_\phi(\mathbf{x}_w)$. The encoder and decoder of HIDDEN are then trained jointly to minimize both the image reconstruction loss (ℓ_{rec}) between \mathbf{x}_w and \mathbf{x} , ensuring visual similarity, and the watermark message decoding loss (ℓ_{dec}), which ensures accurate recovery of the embedded message. This yields the watermark network training problem below

$$\begin{aligned} \psi_w, \phi_w &= \arg \min_{\psi, \phi} \mathcal{L}_{\text{wm}}(\psi, \phi; \mathbf{m}, \mathcal{D}) \\ &:= \mathbb{E}_{\mathbf{x} \in \mathcal{D}} [\ell_{\text{rec}}(\mathbf{x}_w, \mathbf{x}) + \ell_{\text{dec}}(g_\phi(\mathbf{x}_w), \mathbf{m})], \end{aligned} \quad (2)$$

where ψ and ϕ are encoding and decoding network parameters, \mathcal{D} denotes the dataset, and $\mathbf{x}_w = f_\psi(\mathbf{x}, \mathbf{m})$. Once the encoding network is trained by solving (2), we can watermark data by applying $f_{\psi_w}(\mathbf{x}, \mathbf{m})$ to a given data point \mathbf{x} with the specified watermark message \mathbf{m} .

Problem of interest: MU meets watermarking. Our study investigates the synergy between MU and watermarking, serving two primary purposes: (P1) *MU for watermarking*,

which explores the generalizability of MU in unlearning watermarked data; (P2) *Watermarking for MU*, which examines how watermarking can be strategically designed to facilitate effective unlearning.

The rationale behind investigating (P1) is that watermarking can be viewed as a form of data shift, as it introduces alterations to the original dataset. This prompts an examination of whether MU remains generalizable to such shifts during both evaluation and training. Building on the insights gained from exploring (P1), we pose (P2) to examine whether adjustments to the watermarking network in (2) and the selection of the watermark message \mathbf{m} can proactively influence unlearning performance. Here, we aim for a synergistic relationship where watermarking facilitates the MU process, creating a mutually beneficial framework for data watermarking and MU.

4. Generalization of MU to Watermarked Data

In this section, we address (P1) by examining how an off-the-shelf watermarking technique like HIDDEN, when applied to both forget and retain sets, impacts unlearning during training and evaluation. Specifically, given an unlearned model θ_u obtained by solving the unlearning problem (1) on the original (unwatermarked) forget set \mathcal{D}_f , we first assess if the unlearning effectiveness of θ_u generalizes to the watermarked forget set $\hat{\mathcal{D}}_f := \{\mathbf{x}_w\}_{\mathbf{x} \in \mathcal{D}_f}$ and the watermarked retain or testing set at the evaluation phase, where recall that $\mathbf{x}_w = f_{\psi_w}(\mathbf{x}, \mathbf{m})$ as defined in (2). Similarly, if the MU problem (1) is performed on the watermarked dataset, we aim to investigate how its unlearning performance generalizes when evaluated on the *unwatermarked* forget set. The investigation above can be summarized into the following two scenarios of interest (\mathcal{S}_1 - \mathcal{S}_2):

- (\mathcal{S}_1) **Unwatermarked unlearning with watermarked evaluation:** Standard unlearning optimization is performed on the *unwatermarked* dataset, as in (1), while evaluation is conducted on the *watermarked* MU evaluation sets.
- (\mathcal{S}_2) **Watermarked unlearning with unwatermarked evaluation:** Unlearning optimization is applied to the *watermarked* forget and retain sets using the HIDDEN watermarking network ($f_{\psi_w}(\mathbf{x}, \mathbf{m})$), while evaluation is performed on the *unwatermarked* datasets.

Both cases will be validated against the baseline scenario: (\mathcal{S}_0) **unwatermarked unlearning with unwatermarked evaluation.** Our rationale is that comparing \mathcal{S}_1 to \mathcal{S}_0 reveals MU’s robustness to data shifts introduced by watermarking at the testing stage, while comparing \mathcal{S}_2 to \mathcal{S}_0 highlights the impact of watermarking on unlearning training.

To examine the proposed scenarios, we focus on the exact unlearning method of retraining from scratch on the retain set only, referred to as “Retrain”. We did not prioritize approximate unlearning methods to avoid the confounding influence of approximation factors when analyzing the watermarking

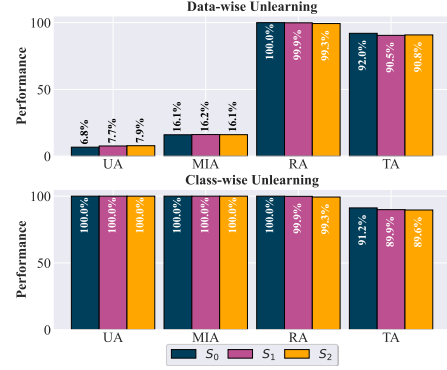


Figure 2. Performance evaluation of the exact unlearning method, Retrain, across the studied MU-watermarking interaction scenarios: \mathcal{S}_1 (unwatermarked unlearning with watermarked evaluation) and \mathcal{S}_2 (watermarked unlearning with unwatermarked evaluation), compared to the unwatermarked baseline \mathcal{S}_0 .

effect in MU. While we acknowledge that Retrain may not be scalable for large datasets, it provides a controlled setting to draw precise insights into the impact of watermarking. To measure *unlearning effectiveness*, we follow [11] and use two metrics: unlearning accuracy (UA), defined as $1 - (\text{accuracy of the unlearned model } \theta_u \text{ on the forget set})$, and MIA-Efficacy, which measures the prediction accuracy of a membership inference attack (MIA)-based detector in correctly identifying the forget data as non-training samples. To assess *model utility* after unlearning, we use retain accuracy (RA) and testing accuracy (TA), which evaluate the prediction accuracy of θ_u on \mathcal{D}_r and the testing set, respectively.

Given the evaluation metrics (UA, MIA-Efficacy, RA, TA), Fig. 2 presents the performance of Retrain under different MU-watermarking interaction scenarios (\mathcal{S}_1 and \mathcal{S}_2) vs. the unwatermarked baseline \mathcal{S}_0 in both data-wise and forget-wise forgetting. As illustrated by the comparison of \mathcal{S}_1 vs. \mathcal{S}_0 , the application of watermarking to unlearning evaluation sets shows negligible impact on the effectiveness of MU, demonstrating its robustness against data modifications introduced by watermarking. Furthermore, in the comparison of \mathcal{S}_2 vs. \mathcal{S}_0 , performing unlearning optimization directly on watermarked datasets also demonstrates minimal impact on the unlearning outcomes. This finding highlights the seamless compatibility of MU methods with watermarked data, ensuring reliable and consistent performance across both standard and watermarked scenarios. This observation further motivates our investigation in the next section, where we explore proactive watermarking design to enhance and facilitate the MU process.

5. WATER4MU: MU Enhanced by Watermark

In this section, we address (P2), as described in Sec. 3, to investigate how the watermarking mechanism in (2) can be strategically designed to proactively facilitate MU when the watermark is applied to the forget data. We refer to the

proposed approach as WATER4MU.

A bi-level optimization (BLO) view of WATER4MU. BLO is used to characterize a leader-follower game [89], in which the leader's actions depend on the optimal solution determined by the follower. If we consider the watermarking procedure conducted by the leader and the unlearning procedure by the follower, we can apply BLO to design the watermarking process in a way that facilitates the unlearning process. Specifically, applying BLO involves two levels of optimization: the *upper-level* optimization, corresponding to the leader's task (*i.e.*, optimization for watermarking), and the *lower-level* optimization, corresponding to the follower's task (*i.e.*, optimization for unlearning). In the following, we detail each optimization level in our proposal, WATER4MU.

We start with the design of the lower-level optimization for unlearning, given the watermarked datasets. Considering the unlearning objective \mathcal{L}_{mu} as formulated in (1), with watermarked data produced by the watermarking encoder f_ψ in (2), the follower in the lower-level optimization seeks to obtain the unlearned model by minimizing \mathcal{L}_{mu} over the watermarked forget and retain sets:

$$\theta_u(\psi) = \arg \min_{\theta} \underbrace{-\ell_{\text{CE}}(\theta; \hat{\mathcal{D}}_f) + \ell_{\text{CE}}(\theta; \hat{\mathcal{D}}_r)}_{=\mathcal{L}_{\text{mu}}(\theta; \hat{\mathcal{D}}_f, \hat{\mathcal{D}}_r)}, \quad (3)$$

where $\hat{\mathcal{D}}_f$ (or $\hat{\mathcal{D}}_r$) denotes the watermarked forget (or retain) dataset, *i.e.*, $\hat{\mathcal{D}}_f := \{\mathbf{x}_w\}_{\mathbf{x} \in \mathcal{D}_f}$ and $\hat{\mathcal{D}}_r := \{\mathbf{x}_w\}_{\mathbf{x} \in \mathcal{D}_r}$ with $\mathbf{x}_w = f_\psi(\mathbf{x}, \mathbf{m})$ in (2). In (3), we explicitly express the minimizer $\theta_u(\psi)$ as a function of the watermarking network parameters ψ . In addition, unless specified otherwise, we define the unlearning objective of (3) by setting $\lambda_f = \lambda_r = 1$, $\ell_r = \ell_{\text{CE}}$, and $\ell_f = -\ell_{\text{CE}}$ in (1). This setup is commonly known as gradient difference method (GradDiff) [4, 90].

Next, we introduce the upper-level optimization for the MU-aware watermarking design. Given the lower-level problem (3), the upper-level optimization has two primary objectives: (a) ensuring that the lower-level unlearned model $\theta_u(\psi)$, trained on watermarked datasets, performs effectively when evaluated on the original unwatermarked datasets, and (b) maintaining the effectiveness of the watermarking network to reliably encode and decode the watermark message. This leads to the following objective:

$$\begin{aligned} \hat{\mathcal{L}}(\psi, \phi, \theta_u(\psi)) := & \underbrace{\mathcal{L}_{\text{mu}}(\theta_u(\psi); \mathcal{D}_f, \mathcal{D}_r)}_{\text{(a) Unlearning validation}} \\ & + \underbrace{\mathcal{L}_{\text{wm}}(\psi, \phi; \mathbf{m}, \mathcal{D}_f \cup \mathcal{D}_r)}_{\text{(b) Watermarking validation}}, \end{aligned} \quad (4)$$

where \mathcal{L}_{mu} is defined in (1) with the GradDiff specification as in (3) in order to validate the lower-level unlearned model $\theta_u(\psi)$ on the original MU dataset, and \mathcal{L}_{wm} represents the training loss of the watermarking network, as defined in (2).

Integrating (4) with (3) forms the proposed BLO problem required for the design of WATER4MU. It is evident from (4) that these two optimization levels are interconnected through the upper-level watermarking encoder parameters ψ , which

influence the lower-level solution $\theta_u(\psi)$. Therefore, the BLO problem for WATER4MU is cast as

$$\begin{aligned} & \underset{\psi, \phi}{\text{minimize}} && \hat{\mathcal{L}}(\psi, \phi, \theta_u(\psi)) \\ & \text{subject to} && \theta_u(\psi) = \arg \min_{\theta} \mathcal{L}_{\text{mu}}(\theta; \hat{\mathcal{D}}_f, \hat{\mathcal{D}}_r), \end{aligned} \quad (5)$$

where $\hat{\mathcal{L}}$ and \mathcal{L}_{mu} have been defined in (3) and (4) respectively, and recall that the watermarked datasets $\hat{\mathcal{D}}_f$ and $\hat{\mathcal{D}}_r$ depend on the upper-level watermarking encoder ψ .

Solving problem (5) via implicit gradient. To solve the BLO problem (5) using a standard gradient descent approach to minimize the upper-level objective function, we face a difficulty known as the implicit gradient (IG) challenge. This arises from the gradient of the upper-level objective, which depends implicitly on the lower-level solution. Specifically, the gradient of the upper-level objective involves:

$$\frac{d\hat{\mathcal{L}}}{d\psi} = \nabla_{\psi} \hat{\mathcal{L}}(\psi, \phi, \theta_u) + \underbrace{\frac{d\theta_u(\psi)}{d\psi}}_{\text{IG}} \nabla_{\theta} \hat{\mathcal{L}}(\psi, \phi, \theta) \big|_{\theta=\theta_u}, \quad (6)$$

where $\nabla_{\psi} \hat{\mathcal{L}}$ or $\nabla_{\theta} \hat{\mathcal{L}}$ denotes the partial derivative ($\frac{\partial}{\partial \cdot}$) of the multi-variate function $\hat{\mathcal{L}}(\psi, \phi, \theta)$, and $\frac{d}{d\cdot}$ denotes the full derivative. In (6), $\frac{d\theta_u(\psi)}{d\psi}$ represents the IG, as $\theta_u(\psi)$ is obtained by solving a coupled but implicit lower-level optimization problem in (5), making its closed-form solution challenging to derive.

To address the IG challenge, we employ a widely used optimization technique known as the *implicit function* approach [89, Sec. III-A]. This approach leverages the Implicit Function Theorem [91], assuming that a singleton solution exists for the lower-level problem. This leads to the following expression of IG:

$$\frac{d\theta_u(\psi)}{d\psi} = -\nabla_{\psi}^2 \ell_{\text{mu}} (\nabla_{\theta\theta}^2 \ell_{\text{mu}})^{-1}, \quad (7)$$

where ℓ_{mu} is the lower-level objective function of (5), we have used and will continue to use omitted input arguments in functions for brevity, $\nabla_{\psi\theta}^2$ denotes the (cross-variable) second-order partial derivative, $\nabla_{\theta\theta}^2$ is the Hessian matrix, and $^{-1}$ is the matrix inversion. To further simplify the IG expression in (7), a common approximation assumes a diagonal matrix for the Hessian. This assumption is reasonable because the prediction loss landscape of deep neural networks is often considered piecewise linear in a tropical hyper-surface [92]. By setting $\nabla_{\theta\theta}^2 \ell_{\text{mu}} = \lambda \mathbf{I}$, where λ is a small hyperparameter to adjust the approximation, we can simplify (7) to:

$$\frac{d\theta_u(\psi)}{d\psi} = -(1/\lambda) \nabla_{\psi\theta}^2 \ell_{\text{mu}}. \quad (8)$$

Substituting (8) into (6), the gradient of the upper-level objective becomes

$$\frac{d\hat{\mathcal{L}}}{d\psi} = \nabla_{\psi} \hat{\mathcal{L}} - \nabla_{\psi\theta}^2 \ell_{\text{mu}} \nabla_{\theta} \hat{\mathcal{L}} = \nabla_{\psi} \hat{\mathcal{L}} - \frac{\partial}{\partial \psi} [\nabla_{\theta} \ell_{\text{mu}}^{\top} \nabla_{\theta} \hat{\mathcal{L}}],$$

where $^\top$ is the transpose of a vector. The above implies that the upper-level gradient calculation to perform gradient descent on (5) can be achieved through the first-order derivatives of two scalar-valued functions, $\hat{\mathcal{L}}$ and $\nabla_{\theta} \ell_{\text{mu}}^T \nabla_{\theta} \hat{\mathcal{L}}$. This allows us to implement WATER4MU using a standard first-order optimization solver to address (5).

WATER4MU in the image generation context. The previously proposed BLO problem was conceived for unlearning in the context of image classification. We can also extend WATER4MU to the prompt-wise forgetting in image generation context. Here, a prompt refers to a text condition used for text-to-image generation, known as a ‘concept’ within MU for generative models [15]. In the lower-level optimization, we conduct unlearning on the prompt with corresponding watermarked forget and retain sets. Then, the upper-level optimization ensures that the unlearned model performs well when evaluated on the unwatermarked datasets and maintains the effectiveness of the watermarking network. See Appx. A for details.

Another extended case: Watermark message (\mathbf{m}) selection. In the standard watermark network training setup, like in HIDDEN, the watermark message \mathbf{m} is treated as a random message. However, given a fixed watermarking network, we can also enhance WATER4MU by selecting a watermark message \mathbf{m} that facilitates MU. This introduces the problem of watermark message selection while keeping the watermark network parameters (ψ, ϕ) unchanged. Analogous to (5), we substitute the upper-level optimization variables with the watermark message variables \mathbf{m} . As shown in (3), the watermark message \mathbf{m} influences the lower-level unlearning objective, thereby serving as the new coupling variable that connects the lower-level optimization to the upper-level optimization. A similar implicit gradient approach can be applied to solve this extended case.

6. Experiments

6.1. Experiment setups

Watermarking and unlearning setups. For watermarking, we use the pre-trained HIDDEN [31] as our baseline watermarking network, which we then fine-tune when integrated with unlearning. For unlearning, we consider three MU scenarios in image classification and image generation. In the *random data* forgetting scenario, we perform primary experiments on the CIFAR-10 dataset using a RESNET-18 model, with additional evaluations on CIFAR-100 and SVHN. In the *class-wise* forgetting scenario, we focus on the CIFAR-10 and IMAGENET datasets, also using a RESNET-18 model. In prompt-wise forgetting, we use UNLEARNCANVAS[9] dataset with the corresponding fine-tuned Stable Diffusion (SD) v1.5. In addition to standard unlearning tasks, we consider a *worst-case* scenario, known as “*challenging forgets*” [93], which identifies data points that are particularly

difficult to unlearn. This approach ranks data based on unlearning difficulty, providing a subset of training samples that present the greatest challenges for unlearning.

Unlearning baseline methods and evaluation metrics.

For image classification, we compare our proposed WATER4MU with the exact unlearning method Retrain and four approximate unlearning methods, FT (fine-tuning) [20], GA (gradient ascent) [22], ℓ_1 sparsity-promoted unlearning (referred to as Sparse) [11], and IU (influence unlearning) [19]. For image generation, we compare WATER4MU with three prompt-wise unlearning methods, erased stable diffusion (ESD)[15], forget-me-not (FMN)[46] and unified concept editing (UCE)[43]. For evaluation, we use four metrics introduced in Sec. 4: UA (unlearning accuracy) and MIA (membership inference attack-based unlearning efficacy) to assess unlearning performance, and RA (accuracy on the retain set) and TA (accuracy on the testing set) to evaluate the utility of the unlearned model. Also for image generation, we have additionally introduced the In-domain retain accuracy (IRA), Cross-domain retain accuracy (CRA), and FID metrics followed the setting of UNLEARNCANVAS[9].

BLO implementation for WATER4MU. For image classification context, in the upper-level optimization, we use the proposed implicit gradient-based descent approach with setting the learning rate to 10^{-4} over 10 epochs. In the lower-level optimization, unlearning is performed with 3 epochs at the learning rate 10^{-2} . The Hessian diagonalization parameter is set to $\lambda = 10^{-2}$. For image generation context, we set the learning rate to 10^{-4} over 6 epochs in the upper-level optimization, while setting the learning rate to 10^{-5} over 5 epochs in the lower-level optimization. The Hessian diagonalization parameter is set to $\lambda = 10^{-2}$. For watermark message selection, we use the same optimization approach as image classification context, while setting the learning rate to $\alpha = 10^{-3}$ over 20 epochs in the upper-level optimization. The Hessian diagonalization parameter is set to $\lambda = 10^{-3}$. All our experiments are conducted on one NVIDIA RTX A6000 48G GPU.

6.2. Experiment results

Effectiveness of WATER4MU-integrated unlearning. In Tab. 1, we present the performance of various MU methods, including the exact unlearning method Retrain and approximate unlearning methods (FT, GA, Sparse, and IU), *with* and *without* the integration of WATER4MU on the (CIFAR-10, ResNet-18) setup. This integration is implemented under scenario \mathcal{S}_{ϵ} —watermarked unlearning with unwatermarked evaluation—as defined in Sec. 4, with the watermarking mechanism provided by WATER4MU. Here our focus on unwatermarked evaluation allows us to examine whether watermarking can enhance MU performance even in evaluations on the original, unwatermarked forget set. We provide several key observations from Tab. 1 below.

Table 1. Performance of different unlearning methods under unwatermarked forget/retain sets (Original) and WATER4MU-induced watermarked forget/retain sets on (CIFAR-10, RESNET-18). The result format is given by $a \pm b$ with mean a and standard deviation b over 10 independent trials. We present the results under random data forgetting and class-wise forgetting scenarios. The forgetting data of random data forgetting ratio is 10% of the whole training dataset. The performance difference is provided in Diff.

Metric	Retrain			GA			FT			Sparse			IU		
	Original	WATER4MU	Diff	Original	WATER4MU	Diff	Original	WATER4MU	Diff	Original	WATER4MU	Diff	Original	WATER4MU	Diff
10% random data forgetting															
UA↑	6.78±0.63	10.01±0.69	3.23▲	0.80±0.32	1.92±0.25	1.12▲	1.85±0.69	4.93±0.76	3.08▲	6.11±0.72	7.50±0.64	1.39▲	0.64±0.21	2.62±0.22	1.98▲
MIA↑	16.06±0.07	19.33±0.05	3.27▲	1.89±0.02	5.67±0.02	3.78▲	5.60±0.22	8.26±0.12	2.66▲	13.08±0.08	14.70±0.02	1.62▲	1.53±0.01	3.67±0.01	2.14▲
RA↑	100.00±0.00	99.93±0.01	0.07▼	99.42±0.27	99.18±0.34	0.24▼	99.66±0.06	98.75±0.10	0.91▼	97.76±0.32	97.22±0.23	0.54▼	99.43±0.22	98.98±0.36	0.45▼
TA↑	92.02±0.02	90.63±0.02	1.39▼	92.19±0.52	92.39±0.38	0.20▲	93.54±0.27	92.11±0.41	1.43▼	91.61±0.46	91.65±0.55	0.04▲	94.51±0.87	92.87±0.74	1.64▼
class-wise forgetting															
UA↑	100.00±0.00	100.00±0.00	0.00-	41.84±7.35	49.03±5.46	7.19▲	37.29±8.18	53.25±6.55	15.96▲	87.09±2.19	94.60±2.02	7.51▲	92.03±2.54	98.49±1.12	6.46▲
MIA↑	100.00±0.00	100.00±0.00	0.00-	55.11±8.32	61.42±7.75	6.31▲	55.96±6.49	69.24±9.17	13.28▲	90.62±2.13	98.71±1.14	8.09▲	99.32±0.21	100.00±0.00	0.68▲
RA↑	100.00±0.00	99.84±0.03	0.16▼	99.20±0.12	99.07±0.23	0.13▼	99.31±0.07	98.76±0.12	0.55▼	99.58±0.05	95.27±0.33	4.31▼	92.27±0.26	92.17±0.41	0.10▼
TA↑	91.20±0.11	89.95±0.21	1.25▼	87.87±0.07	88.62±0.18	0.75▲	90.67±0.22	90.61±0.14	0.06▼	90.48±0.31	90.24±0.10	0.24▼	89.50±0.07	88.67±0.05	0.83▼

Table 2. Performance of WATER4MU on additional datasets in RESNET-18 (CIFAR-10 and SVHN for random data forgetting, IMAGENET for class-wise forgetting). The class-wise forgetting is conducted over 10% of ImageNet classes. The other content format follows Tab. 1.

Metric	Retrain			GA			FT			Sparse			IU		
	Original	WATER4MU	Diff	Original	WATER4MU	Diff	Original	WATER4MU	Diff	Original	WATER4MU	Diff	Original	WATER4MU	Diff
10% random data forgetting, CIFAR-100															
UA↑	24.88±0.13	28.32±0.67	3.44▲	0.05±0.01	2.29±0.12	2.24▲	0.98±0.06	3.11±0.27	2.13▲	9.12±0.21	13.31±0.11	4.19▲	3.19±0.09	5.43±0.33	2.24▲
MIA↑	49.83±0.17	49.96±0.25	0.13▲	2.40±0.21	5.49±0.52	3.09▲	2.29±0.29	5.89±0.32	3.60▲	12.56±0.72	19.64±1.07	7.08▲	6.71±0.40	10.78±0.33	4.07▲
RA↑	99.99±0.01	99.38±0.21	0.61▼	99.97±0.02	99.58±0.09	0.39▼	99.98±0.01	99.91±0.03	0.07▼	96.32±0.07	96.71±0.11	0.39▲	97.86±0.02	97.11±0.03	0.75▼
TA↑	76.35±0.13	73.31±0.22	3.04▼	75.91±0.19	74.43±0.35	1.48▼	75.96±0.27	74.83±0.14	1.13▼	70.43±0.49	69.77±0.26	0.66▼	72.75±0.25	72.53±0.16	0.22▼
10% random data forgetting, SVHN															
UA↑	7.49±0.16	8.79±0.29	1.30▲	0.02±0.01	2.18±0.17	2.16▲	1.98±0.23	4.31±0.20	2.33▲	5.01±0.17	7.66±0.12	2.65▲	4.94±0.12	7.02±0.47	2.08▲
MIA↑	17.77±0.14	17.67±0.15	0.11▼	0.30±0.06	3.67±0.22	3.37▲	5.35±0.19	11.69±0.55	6.34▲	10.62±0.15	13.81±0.38	3.19▲	7.23±0.09	8.96±0.25	1.73▲
RA↑	100.00±0.00	99.95±0.02	0.05▼	99.97±0.01	99.00±0.13	0.97▼	98.98±0.07	99.59±0.11	0.61▲	99.14±0.05	98.57±0.12	0.57▼	99.46±0.02	99.20±0.04	0.26▼
TA↑	93.71±0.42	93.63±0.28	0.08▼	92.59±0.57	92.51±0.18	0.08▼	92.89±0.13	93.40±0.37	0.51▲	93.70±0.08	93.22±0.17	0.48▼	91.13±0.15	90.46±0.11	0.67▼
Class-wise forgetting, IMAGENET															
UA↑	74.33±0.62	76.45±0.49	2.12▲	61.10±0.45	67.23±1.36	6.13▲	45.52±0.86	53.71±0.59	8.19▲	80.25±0.59	85.09±0.37	4.84▲	50.34±0.56	53.71±0.86	3.37▲
MIA↑	98.30±0.17	98.69±0.08	0.39▲	98.71±0.16	99.64±0.22	0.93▲	96.35±0.34	99.56±0.27	3.21▲	98.20±0.20	99.94±0.33	3.21▲	95.78±0.18	95.88±0.13	0.10▲
RA↑	65.80±0.31	64.73±0.29	1.07▼	63.37±0.76	63.05±0.52	0.32▼	65.86±0.46	65.68±0.19	0.18▼	64.34±0.83	62.41±0.08	1.93▼	66.63±0.36	66.24±0.12	0.39▼
TA↑	65.48±0.63	64.21±0.77	1.27▼	63.22±0.47	63.10±0.40	0.12▼	64.89±0.18	64.37±0.52	0.52▼	63.69±0.34	63.22±0.23	0.47▼	65.80±0.24	65.09±0.25	0.71▼

First, integrating WATER4MU into the unlearning process enhances unlearning effectiveness across all evaluated methods, as evidenced by improved UA and MIA scores compared to their performance without WATER4MU (*i.e.*, ‘Original’ in Tab. 1). As noted in Sec. 4, UA is defined as $1 - (\text{accuracy on the forget set } \mathcal{D}_f)$, while the MIA score reflects the accuracy of the MIA detector in correctly identifying forget samples as non-training data. Therefore, an increase in UA and MIA scores indicates more effective unlearning. Another notable observation is that the use of WATER4MU further enhances the unlearning effectiveness of Retrain for data forgetting, indicating the proactive unlearning capability provided by WATER4MU.

Second, we observe that WATER4MU-integrated unlearning approaches result in a slight decrease in model utility, as indicated by RA and TA scores. However, the gains in unlearning effectiveness (evidenced by higher UA and MIA scores) outweigh this slight reduction in TA and RA. This likely reflects the inherent tradeoff between enhanced unlearning effectiveness and preserved model utility [11].

Table 3. Performance of WATER4MU with watermarked evaluation. We choose Retrain as the unlearning method and compare the resulting performance with unwatermarked evaluation under (CIFAR-10, RESNET-18).

Metric	Unwatermarked	Watermarked	Diff
UA↑	10.01±0.69	15.84±1.32	5.83▲
MIA↑	19.33±0.05	26.55±0.15	7.22▲
RA↑	99.93±0.01	97.63±0.76	2.30▼
TA↑	90.63±0.02	88.79±0.55	1.84▼

Third, we observe that integrating WATER4MU is resilient to the choice of MU method. Recall that WATER4MU was designed using the GradDiff unlearning objective in (3), closely aligning with methods like GA and FT. However, integrating WATER4MU with other MU methods, such as Sparse and IU, also enhances unlearning effectiveness, highlighting its broad applicability.

Additional results demonstrating the effectiveness of WATER4MU on other datasets, including CIFAR-100, SVHN, and IMAGENET, are presented in Tab. 2, showing consistent performance trends as observed in Tab. 1.

Effectiveness of WATER4MU in watermarked evaluation. In Tab. 3, we extend the unlearning evaluation of WATER4MU from Tab. 1 to the watermarked evaluation scenario, where the evaluation sets are also watermarked using WATER4MU. As observed, test-time watermarking further enhances unlearning effectiveness (UA and MIA) while slightly reduces utility performance (RA and TA) compared to unwatermarked evaluation. This suggests that watermarking can also serve as an effective test-time strategy to boost MU performance for a given forget set.

Effectiveness of WATER4MU on “challenging forgets” [93]. In Tab. 4, we evaluate the performance of WATER4MU on “challenging forgets”, a worst-case forget set comprising the most difficult training samples or image classes to unlearn. As we can see, integrating WATER4MU into Retrain, GA, and FT shows a clear enhancement in unlearning effectiveness, as evidenced by improved UA and MIA scores

Table 4. Performance of WATER4MU on worst-case challenging forget sets. For data-wise scenarios, we conduct worst-case forgetting on CIFAR-10 using RESNET-18. For class-wise scenarios, we conducted worst-case forgetting on IMAGENET. The data-wise forgetting ratio is 10% of the whole training dataset and the class-wise forgetting ratio is 10% of the entire classes.

Metric	Retrain			GA			FT		
	Original	WATER4MU	Diff	Original	WATER4MU	Diff	Original	WATER4MU	Diff
Worst-case data-wise forgetting, CIFAR-10									
UA↑	0.00±0.00	2.11±0.14	2.11▲	0.01±0.00	1.73±0.02	1.72▲	0.03±0.01	2.05±0.06	2.02▲
MIA↑	0.00±0.00	3.03±0.09	3.03▲	0.33±0.05	2.78±0.13	2.45▲	0.71±0.06	3.40±0.31	2.69▲
RA↑	100.00±0.00	99.87±0.02	0.13▼	99.13±0.03	98.87±0.05	0.26▼	99.66±0.02	99.56±0.02	0.10▼
TA↑	94.78±0.11	94.62±0.23	0.16▼	94.18±0.11	94.38±0.26	0.20▲	94.47±0.17	93.75±0.14	0.72▼
Worst-case class-wise forgetting, IMAGENET									
UA↑	48.49±0.14	51.32±0.33	2.83▲	42.49±0.52	50.21±0.43	7.72▲	33.56±0.06	40.10±0.15	6.54▲
MIA↑	98.63±0.12	98.76±0.21	0.13▲	98.25±0.14	99.47±0.17	1.22▲	96.56±0.26	99.82±0.08	3.26▲
RA↑	65.62±0.41	64.96±0.28	0.66▼	62.83±0.20	62.54±0.44	0.29▼	66.85±0.35	66.52±0.18	0.33▼
TA↑	65.59±0.14	65.31±0.57	0.28▼	63.14±0.15	63.20±0.29	0.06▼	65.73±0.28	64.35±0.72	1.38▼

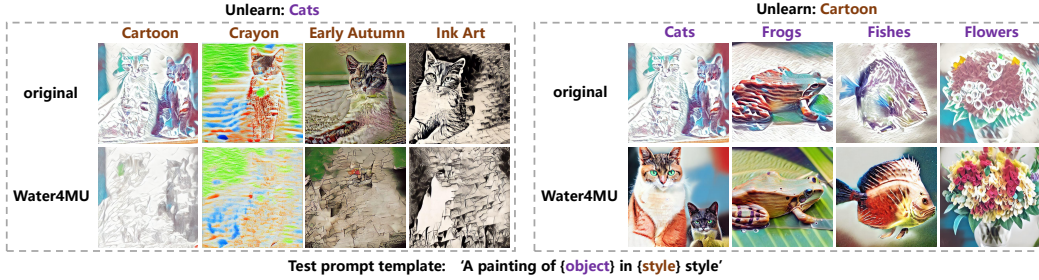


Figure 3. Examples of generated images by SD w/ and w/o MU with WATER4MU. Concept types are distinguished by color: **styles** in brown and **objects** in purple. The first row serves as a reference for comparison before unlearning.

across all datasets. Comparing these results with random data forgetting on CIFAR-10 in Tab. 1 and standard class-wise forgetting on ImageNet in Tab. 2, we observe that unlearning becomes notably more challenging in the worst-case scenario in Tab. 4. Nevertheless, WATER4MU provides a promising solution to further improve existing MU methods, even in these challenging unlearning scenarios.

An extended study: effectiveness of WATER4MU in image generation. We further demonstrate the efficacy of our approach in prompt-wise forgetting for text-to-image generation. We use the Stable Diffusion (SD) model [94] on the UNLEARNCANVAS dataset [9], a benchmark dataset designed to evaluate the unlearning of painting styles and objects. In UnlearnCanvas, a text prompt used as the condition of image generation is given by ‘A painting of [Object Name] in [Style Name] Style.’. We consider 20 objects and 50 styles for unlearning. In Tab. 5, we provide an overview of the performance of WATER4MU, using the evaluation metrics associated with UnlearnCanvas. **First**, as seen in

Table 5. Performance overview of WATER4MU evaluated on UNLEARNCANVAS. The performance metrics include UA (unlearning accuracy), IRA (in-domain retain accuracy), CRA (cross-domain retain accuracy), and FID. Results are averaged over all the style and object unlearning cases.

Metric	Style Unlearning			Object Unlearning			FID↓
	UA↑	IRA↑	CRA↑	UA↑	IRA↑	CRA↑	
ESD	98.58	80.97	93.96	92.15	55.78	44.23	65.55
FMN	88.48	56.77	46.60	45.64	90.63	73.46	131.37
UCE	98.40	60.22	47.71	94.31	39.35	34.67	182.01
Ours	93.49	92.75	94.01	82.24	85.60	81.52	86.62

Tab. 5, we observe that WATER4MU keeps high UA in both style and object unlearning (95% and 82%). **Second**, retainability of WATER4MU is maintained at a high level. Both IRA and CRA exceeds 80% in the context of style and object unlearning. Compared to other MU methods, WATER4MU achieves the best balance between unlearning effectiveness and retainability. **Third**, WATER4MU manages to maintain good generation quality (measured by FID). The above results indicates that WATER4MU can be effectively adapted to prompt-wise unlearning tasks. Fig. A4 showcases the visualizations of the generations produced by unlearned SD with WATER4MU. As observed, WATER4MU achieves effective concept erasure in both style and object unlearning.

Ablation studies. In Appx. C, we provide computational costs of WATER4MU, a hyperparameter sensitivity analysis, the decoding performance of WATER4MU, and the influence of different watermark message selection.

7. Conclusion

In this work, we present WATER4MU, a novel machine unlearning (MU)-aware watermarking framework that introduces a data-centric approach to enhance unlearning effectiveness in image classification. By integrating digital watermarking into MU workflows, WATER4MU complements existing model-centric unlearning methods, showcasing how watermarking can act as a powerful tool for controlled data erasure. Our findings demonstrate that WATER4MU significantly improves unlearning effectiveness across diverse MU methods, including under “challenging forgets” scenarios.

References

- [1] Lucas Bourtole, Varun Chandrasekaran, Christopher A Choquette-Choo, Hengrui Jia, Adelin Travers, Baiwu Zhang, David Lie, and Nicolas Papernot. Machine unlearning. In *2021 IEEE Symposium on Security and Privacy (SP)*, pages 141–159. IEEE, 2021. 1
- [2] Thanh Tam Nguyen, Thanh Trung Huynh, Phi Le Nguyen, Alan Wee-Chung Liew, Hongzhi Yin, and Quoc Viet Hung Nguyen. A survey of machine unlearning. *arXiv preprint arXiv:2209.02299*, 2022.
- [3] Eleni Triantafillou, Peter Kairouz, Fabian Pedregosa, Jamie Hayes, Meghdad Kurmanji, Kairan Zhao, Vincent Dumoulin, Julio Jacques Junior, Ioannis Mitliagkas, Jun Wan, et al. Are we making progress in unlearning? findings from the first neurips unlearning competition. *arXiv preprint arXiv:2406.09073*, 2024. 3
- [4] Sijia Liu, Yuanshun Yao, Jinghan Jia, Stephen Casper, Nathalie Baracaldo, Peter Hase, Xiaojun Xu, Yuguang Yao, Hang Li, Kush R Varshney, et al. Rethinking machine unlearning for large language models. *arXiv preprint arXiv:2402.08787*, 2024. 1, 5
- [5] Chris Conley. The right to delete. In *2010 AAAI Spring Symposium Series*, 2010. 1
- [6] Yinzhi Cao and Junfeng Yang. Towards making systems forget with machine unlearning. In *2015 IEEE Symposium on Security and Privacy*, pages 463–480. IEEE, 2015. 2
- [7] Yonghao Tang, Zhiping Cai, Qiang Liu, Tongqing Zhou, and Qiang Ni. Ensuring user privacy and model security via machine unlearning: A review. *Computers, Materials & Continua*, 77(2), 2023.
- [8] Guangyao Dou, Zheyuan Liu, Qing Lyu, Kaize Ding, and Eric Wong. Avoiding copyright infringement via machine unlearning. *arXiv preprint arXiv:2406.10952*, 2024.
- [9] Yihua Zhang, Yimeng Zhang, Yuguang Yao, Jinghan Jia, Jiancheng Liu, Xiaoming Liu, and Sijia Liu. Unlearncanvas: A stylized image dataset to benchmark machine unlearning for diffusion models. *NeurIPS*, 2024. 1, 2, 6, 8
- [10] Saachi Jain, Hadi Salman, Alaa Khaddaj, Eric Wong, Sung Min Park, and Aleksander Madry. A data-based perspective on transfer learning. In *Proceedings of the IEEE/CVF Conference on Computer Vision and Pattern Recognition*, pages 3613–3622, 2023. 1
- [11] Jinghan Jia, Jiancheng Liu, Parikshit Ram, Yuguang Yao, Gaowen Liu, Yang Liu, Pranay Sharma, and Sijia Liu. Model sparsity can simplify machine unlearning. *Advances in neural information processing systems*, 36, 2023. 1, 2, 3, 4, 6, 7
- [12] Yang Liu, Mingyuan Fan, Cen Chen, Ximeng Liu, Zhuo Ma, Li Wang, and Jianfeng Ma. Backdoor defense with machine unlearning. *arXiv preprint arXiv:2201.09538*, 2022. 1
- [13] Chen Wu, Sencun Zhu, Prasenjit Mitra, and Wei Wang. Unlearning backdoor attacks in federated learning. In *2024 IEEE Conference on Communications and Network Security (CNS)*, pages 1–9. IEEE, 2024. 1
- [14] Zheyuan Liu, Guangyao Dou, Zhaoxuan Tan, Yijun Tian, and Meng Jiang. Towards safer large language models through machine unlearning. *arXiv preprint arXiv:2402.10058*, 2024. 1
- [15] Rohit Gandikota, Joanna Materzynska, Jaden Fiotto-Kaufman, and David Bau. Erasing concepts from diffusion models. *arXiv preprint arXiv:2303.07345*, 2023. 2, 6
- [16] Yimeng Zhang, Xin Chen, Jinghan Jia, Yihua Zhang, Chongyu Fan, Jiancheng Liu, Mingyi Hong, Ke Ding, and Sijia Liu. Defensive unlearning with adversarial training for robust concept erasure in diffusion models. *NeurIPS*, 2024. 1
- [17] Jie Xu, Zihan Wu, Cong Wang, and Xiaohua Jia. Machine unlearning: Solutions and challenges. *IEEE Transactions on Emerging Topics in Computational Intelligence*, 2024. 1
- [18] Zheyuan Liu, Guangyao Dou, Zhaoxuan Tan, Yijun Tian, and Meng Jiang. Machine unlearning in generative ai: A survey. *arXiv preprint arXiv:2407.20516*, 2024. 1
- [19] Zachary Izzo, Mary Anne Smart, Kamalika Chaudhuri, and James Zou. Approximate data deletion from machine learning models. In *International Conference on Artificial Intelligence and Statistics*, pages 2008–2016. PMLR, 2021. 2, 6
- [20] Aditya Golatkar, Alessandro Achille, and Stefano Soatto. Eternal sunshine of the spotless net: Selective forgetting in deep networks. In *Proceedings of the IEEE/CVF Conference on Computer Vision and Pattern Recognition*, pages 9304–9312, 2020. 2, 3, 6
- [21] Alexander Becker and Thomas Liebig. Evaluating machine unlearning via epistemic uncertainty. *arXiv preprint arXiv:2208.10836*, 2022. 3
- [22] Anvith Thudi, Gabriel Deza, Varun Chandrasekaran, and Nicolas Papernot. Unrolling sgd: Understanding factors influencing machine unlearning. In *2022 IEEE 7th European Symposium on Security and Privacy (EuroS&P)*, pages 303–319. IEEE, 2022. 2, 3, 6
- [23] Alexander Warnecke, Lukas Pirch, Christian Wressnegger, and Konrad Rieck. Machine unlearning of features and labels. *arXiv preprint arXiv:2108.11577*, 2021. 2, 3
- [24] Meghdad Kurmanji, Peter Triantafillou, Jamie Hayes, and Eleni Triantafillou. Towards unbounded machine unlearning. *Advances in neural information processing systems*, 36, 2024.
- [25] Chongyu Fan, Jiancheng Liu, Yihua Zhang, Dennis Wei, Eric Wong, and Sijia Liu. Salun: Empowering machine unlearning via gradient-based weight saliency in both image classification and generation. *arXiv preprint arXiv:2310.12508*, 2023. 2
- [26] Jiang Xuehua. Digital watermarking and its application in image copyright protection. In *2010 International Conference on Intelligent Computation Technology and Automation*, volume 2, pages 114–117. IEEE, 2010. 2, 3
- [27] Xuanyu Zhang, Runyi Li, Jiwen Yu, Youmin Xu, Weiqi Li, and Jian Zhang. Editguard: Versatile image watermarking for tamper localization and copyright protection. In *Proceedings of the IEEE/CVF Conference on Computer Vision and Pattern Recognition*, pages 11964–11974, 2024.
- [28] Khalid M Hosny, Amal Magdi, Osama ElKomy, and Hanaa M Hamza. Digital image watermarking using deep learning: A survey. *Computer Science Review*, 53:100662, 2024. 2, 3
- [29] Frank Y Shih and Scott YT Wu. Combinational image watermarking in the spatial and frequency domains. *Pattern Recognition*, 36(4):969–975, 2003. 2

- [30] Deepayan Bhowmik, Matthew Oakes, and Charith Abhayaratne. Visual attention-based image watermarking. *IEEE Access*, 4:8002–8018, 2016.
- [31] Jiren Zhu, Russell Kaplan, Justin Johnson, and Li Fei-Fei. Hidden: Hiding data with deep networks. In *Proceedings of the European conference on computer vision (ECCV)*, pages 657–672, 2018. 2, 3, 6
- [32] Xiyang Luo, Ruohan Zhan, Huiwen Chang, Feng Yang, and Peyman Milanfar. Distortion agnostic deep watermarking. In *Proceedings of the IEEE/CVF conference on computer vision and pattern recognition*, pages 13548–13557, 2020.
- [33] Himanshu Kumar Singh and Amit Kumar Singh. Digital image watermarking using deep learning. *Multimedia Tools and Applications*, 83(1):2979–2994, 2024. 2
- [34] Xin Zhong, Arjon Das, Fahad Alrasheedi, and Abdullah Tanvir. A brief yet in-depth survey of deep learning-based image watermarking. *arXiv preprint arXiv:2308.04603*, 2023. 2
- [35] Antonio Ginart, Melody Guan, Gregory Valiant, and James Y Zou. Making ai forget you: Data deletion in machine learning. *Advances in neural information processing systems*, 32, 2019. 2
- [36] Seth Neel, Aaron Roth, and Saeed Sharifi-Malvajerdi. Descent-to-delete: Gradient-based methods for machine unlearning. In *Algorithmic Learning Theory*, pages 931–962. PMLR, 2021.
- [37] Ayush Sekhari, Jayadev Acharya, Gautam Kamath, and Ananda Theertha Suresh. Remember what you want to forget: Algorithms for machine unlearning. *Advances in Neural Information Processing Systems*, 34:18075–18086, 2021.
- [38] Enayat Ullah, Tung Mai, Anup Rao, Ryan A Rossi, and Raman Arora. Machine unlearning via algorithmic stability. In *Conference on Learning Theory*, pages 4126–4142. PMLR, 2021. 2
- [39] Anvith Thudi, Hengrui Jia, Ilia Shumailov, and Nicolas Papernot. On the necessity of auditable algorithmic definitions for machine unlearning. In *31st USENIX Security Symposium (USENIX Security 22)*, pages 4007–4022, 2022. 2
- [40] Cynthia Dwork, Krishnaram Kenthapadi, Frank McSherry, Ilya Mironov, and Moni Naor. Our data, ourselves: Privacy via distributed noise generation. In *Annual international conference on the theory and applications of cryptographic techniques*, pages 486–503. Springer, 2006. 2
- [41] Laura Graves, Vineel Nagisetty, and Vijay Ganesh. Amnesiac machine learning. In *Proceedings of the AAAI Conference on Artificial Intelligence*, volume 35, pages 11516–11524, 2021. 2
- [42] Chuan Guo, Tom Goldstein, Awni Hannun, and Laurens Van Der Maaten. Certified data removal from machine learning models. *arXiv preprint arXiv:1911.03030*, 2019. 2
- [43] Rohit Gandikota, Hadas Orgad, Yonatan Belinkov, Joanna Materzyńska, and David Bau. Unified concept editing in diffusion models. In *Proceedings of the IEEE/CVF Winter Conference on Applications of Computer Vision*, pages 5111–5120, 2024. 2, 6
- [44] Alvin Heng and Harold Soh. Selective amnesia: A continual learning approach to forgetting in deep generative models, 2023.
- [45] Nupur Kumari, Bingliang Zhang, Sheng-Yu Wang, Eli Shechtman, Richard Zhang, and Jun-Yan Zhu. Ablating concepts in text-to-image diffusion models, 2023.
- [46] Eric Zhang, Kai Wang, Xingqian Xu, Zhangyang Wang, and Humphrey Shi. Forget-me-not: Learning to forget in text-to-image diffusion models. *arXiv preprint arXiv:2303.17591*, 2023. 2, 6
- [47] Tianshi Che, Yang Zhou, Zijie Zhang, Lingjuan Lyu, Ji Liu, Da Yan, Dejing Dou, and Jun Huan. Fast federated machine unlearning with nonlinear functional theory. 2023. 2
- [48] Junxiao Wang, Song Guo, Xin Xie, and Heng Qi. Federated unlearning via class-discriminative pruning. In *Proceedings of the ACM Web Conference 2022*, pages 622–632, 2022.
- [49] Leijie Wu, Song Guo, Junxiao Wang, Zicong Hong, Jie Zhang, and Yaohong Ding. Federated unlearning: Guarantee the right of clients to forget. *IEEE Network*, 36(5):129–135, 2022. 2
- [50] Ronen Eldan and Mark Russinovich. Who’s harry potter? approximate unlearning in llms, 2023. 2
- [51] Xinwei Wu, Junzhuo Li, Minghui Xu, Weilong Dong, Shuangzhi Wu, Chao Bian, and Deyi Xiong. Depn: Detecting and editing privacy neurons in pretrained language models. *arXiv preprint arXiv:2310.20138*, 2023.
- [52] Yuanshun Yao, Xiaojun Xu, and Yang Liu. Large language model unlearning. *arXiv preprint arXiv:2310.10683*, 2023.
- [53] Charles Yu, Sullam Jeoung, Anish Kasi, Pengfei Yu, and Heng Ji. Unlearning bias in language models by partitioning gradients. In *Findings of the Association for Computational Linguistics: ACL 2023*, pages 6032–6048, 2023. 2
- [54] Ingemar Cox, Matthew Miller, Jeffrey Bloom, Jessica Fridrich, and Ton Kalker. *Digital watermarking and steganography*. Morgan kaufmann, 2007. 2
- [55] Matthew L Miller, Ingemar J Cox, and Jeffrey A Bloom. Informed embedding: exploiting image and detector information during watermark insertion. In *Proceedings 2000 International Conference on Image Processing (Cat. No. 00CH37101)*, volume 3, pages 1–4. IEEE, 2000.
- [56] Sviatoslav Voloshynovskiy, Shelby Pereira, Thierry Pun, Joachim J Eggers, and Jonathan K Su. Attacks on digital watermarks: classification, estimation based attacks, and benchmarks. *IEEE communications Magazine*, 39(8):118–126, 2001. 2
- [57] Alessandro Piva, Mauro Barni, Franco Bartolini, and Vito Cappellini. Dct-based watermark recovering without resorting to the uncorrupted original image. In *Proceedings of international conference on image processing*, volume 1, pages 520–523. IEEE, 1997. 2
- [58] Mauro Barni, Franco Bartolini, Vito Cappellini, and Alessandro Piva. A dct-domain system for robust image watermarking. *Signal processing*, 66(3):357–372, 1998. 2
- [59] Xiang-Gen Xia, Charles G Bonchelet, and Gonzalo R Arce. A multiresolution watermark for digital images. In *Proceedings of international conference on image processing*, volume 1, pages 548–551. IEEE, 1997. 2
- [60] Ruizhen Liu and Tieniu Tan. An svd-based watermarking scheme for protecting rightful ownership. *IEEE transactions on multimedia*, 4(1):121–128, 2002. 2

- [61] Kevin Alex Zhang, Alfredo Cuesta-Infante, Lei Xu, and Kalyan Veeramachaneni. Steganogan: High capacity image steganography with gans. *arXiv preprint arXiv:1901.03892*, 2019. 2
- [62] Xiaoshuai Wu, Xin Liao, Bo Ou, Yuling Liu, and Zheng Qin. Are watermarks bugs for deepfake detectors? rethinking proactive forensics. *arXiv preprint arXiv:2404.17867*, 2024. 2
- [63] Yuguang Yao, Steven Grosz, Sijia Liu, and Anil Jain. Hide and seek: How does watermarking impact face recognition? *arXiv preprint arXiv:2404.18890*, 2024. 2
- [64] Hyojin Bahng, Ali Jahanian, Swami Sankaranarayanan, and Phillip Isola. Exploring visual prompts for adapting large-scale models. *arXiv preprint arXiv:2203.17274*, 1(3):4, 2022. 3
- [65] Menglin Jia, Luming Tang, Bor-Chun Chen, Claire Cardie, Serge Belongie, Bharath Hariharan, and Ser-Nam Lim. Visual prompt tuning. *arXiv preprint arXiv:2203.12119*, 2022. 3
- [66] Gamaleldin F Elsayed, Ian Goodfellow, and Jascha Sohl-Dickstein. Adversarial reprogramming of neural networks. *arXiv preprint arXiv:1806.11146*, 2018. 3
- [67] Pin-Yu Chen. Model reprogramming: Resource-efficient cross-domain machine learning. *arXiv preprint arXiv:2202.10629*, 2022.
- [68] Paarth Neekhara, Shehzeen Hussain, Shlomo Dubnov, and Farinaz Koushanfar. Adversarial reprogramming of text classification neural networks. *arXiv preprint arXiv:1809.01829*, 2018.
- [69] Paarth Neekhara, Shehzeen Hussain, Jinglong Du, Shlomo Dubnov, Farinaz Koushanfar, and Julian McAuley. Cross-modal adversarial reprogramming. In *Proceedings of the IEEE/CVF Winter Conference on Applications of Computer Vision*, pages 2427–2435, 2022.
- [70] Lingwei Chen, Yujie Fan, and Yanfang Ye. Adversarial reprogramming of pretrained neural networks for fraud detection. In *Proceedings of the 30th ACM International Conference on Information & Knowledge Management*, pages 2935–2939, 2021. 3
- [71] Guanhua Zhang, Yihua Zhang, Yang Zhang, Wenqi Fan, Qing Li, Sijia Liu, and Shiyu Chang. Fairness reprogramming. *Advances in Neural Information Processing Systems*, 35:34347–34362, 2022.
- [72] Aochuan Chen, Peter Lorenz, Yuguang Yao, Pin-Yu Chen, and Sijia Liu. Visual prompting for adversarial robustness. *arXiv preprint arXiv:2210.06284*, 2022.
- [73] Quanwei Yang, Jiazhi Guan, Kaisiyuan Wang, Lingyun Yu, Wenqing Chu, Hang Zhou, ZhiQiang Feng, Haocheng Feng, Errui Ding, Jingdong Wang, and Hongtao Xie. Showmaker: Creating high-fidelity 2d human video via fine-grained diffusion modeling. In *NeurIPS*, 2024. 3
- [74] Ziqing Yang, Zeyang Sha, Michael Backes, and Yang Zhang. From visual prompt learning to zero-shot transfer: Mapping is all you need. *arXiv preprint arXiv:2303.05266*, 2023. 3
- [75] Junyang Wu, Xianhang Li, Chen Wei, Huiyu Wang, Alan Yuille, Yuyin Zhou, and Cihang Xie. Unleashing the power of visual prompting at the pixel level. *arXiv preprint arXiv:2212.10556*, 2022. 3
- [76] Aochuan Chen, Peter Lorenz, Yuguang Yao, Pin-Yu Chen, and Sijia Liu. Visual prompting for adversarial robustness. In *ICASSP 2023-2023 IEEE International Conference on Acoustics, Speech and Signal Processing (ICASSP)*, pages 1–5. IEEE, 2023. 3
- [77] Chengzhi Mao, Scott Geng, Junfeng Yang, Xin Wang, and Carl Vondrick. Understanding zero-shot adversarial robustness for large-scale models. *arXiv preprint arXiv:2212.07016*, 2022. 3
- [78] Yizhe Li, Yu-Lin Tsai, Chia-Mu Yu, Pin-Yu Chen, and Xuebin Ren. Exploring the benefits of visual prompting in differential privacy. In *Proceedings of the IEEE/CVF International Conference on Computer Vision*, pages 5158–5167, 2023. 3
- [79] Can Jin, Tianjin Huang, Yihua Zhang, Mykola Pechenizkiy, Sijia Liu, Shiwei Liu, and Tianlong Chen. Visual prompting upgrades neural network sparsification: A data-model perspective. *arXiv preprint arXiv:2312.01397*, 2023. 3
- [80] Xinhong Ma, Yiming Wang, Hao Liu, Tianyu Guo, and Yunhe Wang. When visual prompt tuning meets source-free domain adaptive semantic segmentation. *Advances in Neural Information Processing Systems*, 36, 2024. 3
- [81] Yihua Zhang, Hongkang Li, Yuguang Yao, Aochuan Chen, Shuai Zhang, Pin-Yu Chen, Meng Wang, and Sijia Liu. Visual prompting reimaged: The power of activation prompts. 2024. 3
- [82] Qidong Huang, Xiaoyi Dong, Dongdong Chen, Weiming Zhang, Feifei Wang, Gang Hua, and Nenghai Yu. Diversity-aware meta visual prompting. In *Proceedings of the IEEE/CVF Conference on Computer Vision and Pattern Recognition*, pages 10878–10887, 2023. 3
- [83] Yun-Yun Tsai, Chengzhi Mao, Yow-Kuan Lin, and Junfeng Yang. Self-supervised convolutional visual prompts. *arXiv preprint arXiv:2303.00198*, 2023. 3
- [84] Kaiyang Zhou, Jingkang Yang, Chen Change Loy, and Ziwei Liu. Learning to prompt for vision-language models. *International Journal of Computer Vision*, 130(9):2337–2348, 2022. 3
- [85] Junda Wu, Zhehao Zhang, Yu Xia, Xintong Li, Zhaoyang Xia, Aaron Chang, Tong Yu, Sungchul Kim, Ryan A Rossi, Ruiyi Zhang, et al. Visual prompting in multimodal large language models: A survey. *arXiv preprint arXiv:2409.15310*, 2024.
- [86] Nilakshan Kunanathaseelan, Jing Zhang, and Mehrtaash Harandi. Lavip: Language-grounded visual prompting. In *Proceedings of the AAAI Conference on Artificial Intelligence*, volume 38, pages 2840–2848, 2024. 3
- [87] Kristian Georgiev, Roy Rinberg, Sung Min Park, Shivam Garg, Andrew Ilyas, Aleksander Madry, and Seth Neel. Attribute-to-delete: Machine unlearning via datamodel matching. *arXiv preprint arXiv:2410.23232*, 2024. 3
- [88] Min Chen, Weizhuo Gao, Gaoyang Liu, Kai Peng, and Chen Wang. Boundary unlearning: Rapid forgetting of deep networks via shifting the decision boundary. In *Proceedings of the IEEE/CVF Conference on Computer Vision and Pattern Recognition*, pages 7766–7775, 2023. 3
- [89] Yihua Zhang, Prashant Khanduri, Ioannis Tsaknakis, Yuguang Yao, Mingyi Hong, and Sijia Liu. An introduction to bilevel optimization: Foundations and applications in signal

- processing and machine learning. *IEEE Signal Processing Magazine*, 41(1):38–59, 2024. [5](#)
- [90] Pratyush Maini, Zhili Feng, Avi Schwarzschild, Zachary C. Lipton, and J. Zico Kolter. Tofu: A task of fictitious unlearning for llms, 2024. [5](#)
- [91] Steven George Krantz and Harold R Parks. *The implicit function theorem: history, theory, and applications*. Springer Science & Business Media, 2002. [5](#)
- [92] Motasem Alfarra, Adel Bibi, Hasan Hammoud, Mohamed Gaafar, and Bernard Ghanem. On the decision boundaries of neural networks: A tropical geometry perspective. *IEEE Transactions on Pattern Analysis and Machine Intelligence*, 45(4):5027–5037, 2022. [5](#)
- [93] Chongyu Fan, Jiancheng Liu, Alfred Hero, and Sijia Liu. Challenging forgets: Unveiling the worst-case forget sets in machine unlearning. In *European Conference on Computer Vision*, pages 278–297. Springer, 2025. [6](#), [7](#)
- [94] Robin Rombach, Andreas Blattmann, Dominik Lorenz, Patrick Esser, and Björn Ommer. High-resolution image synthesis with latent diffusion models. In *Proceedings of the IEEE/CVF Conference on Computer Vision and Pattern Recognition*, pages 10684–10695, 2022. [8](#)

Appendix

A. BLO framework of WATER4MU for image generation

In the context of prompt-wise forgetting in image generation, the BLO problem for WATER4MU can be also cast as (5):

$$\begin{aligned} & \underset{\psi, \phi}{\text{minimize}} && \hat{\mathcal{L}}(\psi, \phi, \theta_u(\psi)) \\ & \text{subject to} && \theta_u(\psi) = \arg \min_{\theta} \mathcal{L}_{\text{mu}}(\theta; \hat{\mathcal{D}}_f, \hat{\mathcal{D}}_r), \end{aligned} \quad (\text{A1})$$

In the lower-level optimization, we first obtain the watermarked dataset for unlearning. Then, we extend the use of Random Label (RL) to the image generation context for unlearning concept c . Also, to maintain the generation capability of the model, we introduce the regularization loss on the watermarked retain set. Finally, we can obtain an unlearned model θ_u :

$$\begin{aligned} \theta_u(\psi) = \arg \min_{\theta} & \mathbb{E}_{\mathbf{x} \in \hat{\mathcal{D}}_f, t, \epsilon} [\|\epsilon_{\theta}(x_t|c') - \epsilon_{\theta}(x_t|c)\|_2^2] \\ & + \mathbb{E}_{\mathbf{x} \in \hat{\mathcal{D}}_r, t, \epsilon} [\|\epsilon - \epsilon_{\theta}(x_t|c_r)\|_2^2], \end{aligned} \quad (\text{A2})$$

where $c' \neq c$, c_r is the prompt of $x \in \hat{\mathcal{D}}_r$, $\hat{\mathcal{D}}_f$ (or $\hat{\mathcal{D}}_r$) denotes the watermarked forget (or retain) dataset, θ is the pretrained generative model and β is a regularization parameter.

The design of the upper-level optimization follows (4):

$$\begin{aligned} \hat{\mathcal{L}}(\psi, \phi, \theta_u(\psi)) := & \underbrace{\mathcal{L}_{\text{mu}}(\theta_u(\psi); \mathcal{D}_f, \mathcal{D}_r)}_{\text{(a) Unlearning validation}} \\ & + \underbrace{\mathcal{L}_{\text{wm}}(\psi, \phi; \mathbf{m}, \mathcal{D}_f \cup \mathcal{D}_r)}_{\text{(b) Watermarking validation}}, \end{aligned} \quad (\text{A3})$$

where ℓ_{mu} is defined in (A2) and $\mathcal{L}_{\text{mu}}(\theta_u(\psi); \mathcal{D}_f, \mathcal{D}_r)$ is to validate the lower-level unlearned model $\theta_u(\psi)$ on the unwatermarked dataset, and ℓ_{wm} is the training loss of the watermarking network.

B. Additional Experiment Setup

B.1. WATER4MU for image classification

For the exact unlearning method Retrain, the training process comprises 182 epochs, utilizing the SGD optimizer with a cosine-scheduled learning rate initially set to 0.1. For FT, the unlearning process takes 10 epochs, during which the optimal learning rate is searched within the range of $[10^{-3}, 10^{-1}]$. For GA, the unlearning process spans 5 epochs with the interval $[10^{-5}, 10^{-3}]$. Regarding the method Sparse, the unlearning-enabled model updating process also takes 10 epochs, searching the optimal sparse ratio in the range $[10^{-6}, 10^{-4}]$ and exploring learning rate within $[10^{-3}, 10^{-1}]$. Finally, for IU, the parameter α (associated with the Wood-Fisher Hessian Inverse approximation) is searched within the range $[1, 20]$.

B.2. WATER4MU for image generation

We follow the settings in the UNLEARNCANVAS benchmark, selecting 20 objects and 50 styles for unlearning. The β is set at 0.5, with a batch size of 1. The sampling settings involve the use of DDPM, 100 time steps, and a conditional scale of 7.5.

C. Additional Experiment Results

C.1. Ablation study

The computational costs of WATER4MU. We measure the run-time efficiency (RTE) of applying an MU method, *i.e.*, its computation time. In Tab. A1, we compared the RTE of different methods with and without using WATER4MU on (CIFAR-10, RESNET-18). As we can see, the introduction of WATER4MU does not hamper the computation efficiency, highlighting its practicality.

Table A1. Performance of RTE (min) of different unlearning methods under unwatermarked forget/retain sets (Original) and WATER4MU-induced watermarked forget/retain sets on (CIFAR-10, RESNET-18) for class-wise forgetting.

MU	Retrain	GA	FT	Sparse	IU
Original	42.35	0.25	2.50	2.52	3.25
WATER4MU	49.93	0.30	3.07	3.09	3.98

Choice of λ in diagonalization approximation of the Hessian matrix. We next examine the hyperparameter λ in Hessian’s diagonalization approximation in (8) for WATER4MU. In our experiments, the default setting is $\lambda = 10^{-2}$. We conduct a more detailed examination of λ in Fig. A1. We can observe that $\lambda = 10^{-2}$ is a reasonable option, and higher or lower value of λ would reduce the effectiveness of WATER4MU.

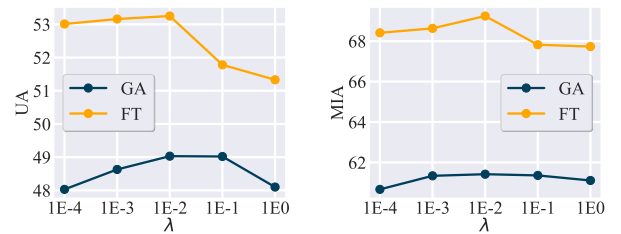


Figure A1. Unlearning effectiveness (in terms of UA and MIA) of GA and FT against the choice of λ in WATER4MU for class-wise forgetting under (CIFAR-10, RESNET-18).

Decoding performance of WATER4MU. While WATER4MU enhances the unlearning effectiveness, the decoding performance of WATER4MU as a watermarking method should also be maintained. We then use BER (Bit Error Rate) to measure the performance of WATER4MU to decode

Table A2. Performance of different unlearning methods under unwatermarked forget/retain sets (Original) and WATER4MU-induced watermarked forget/retrain sets on (CIFAR-100, RESNET-18) and (SVHN, RESNET-18) for class-wise forgetting.

Metric	Retrain			GA			FT		
	Original	WATER4MU	Diff	Original	WATER4MU	Diff	Original	WATER4MU	Diff
Class-wise forgetting, RESNET-18, CIFAR-100									
UA	100.00 \pm 0.00	100.00 \pm 0.00	0.00-	83.67 \pm 0.78	90.46 \pm 0.43	6.33 \blacktriangle	24.73 \pm 2.63	29.56 \pm 2.78	4.83 \blacktriangle
MIA	100.00 \pm 0.00	100.00 \pm 0.00	0.00-	91.51 \pm 2.66	98.22 \pm 0.12	6.71 \blacktriangle	45.61 \pm 0.3.31	50.36 \pm 2.09	4.75 \blacktriangle
RA	99.98 \pm 0.01	98.87 \pm 0.05	1.11 \blacktriangledown	91.56 \pm 0.54	88.32 \pm 1.18	3.24 \blacktriangledown	99.18 \pm 0.26	99.03 \pm 0.72	0.15 \blacktriangledown
TA	74.43 \pm 0.23	72.89 \pm 0.13	0.16 \blacktriangledown	65.79 \pm 0.69	64.61 \pm 0.19	1.18 \blacktriangledown	74.33 \pm 0.14	72.50 \pm 0.27	1.83 \blacktriangledown
Class-wise forgetting, RESNET-18, SVHN									
UA	100.00 \pm 0.00	100.00 \pm 0.00	0.00-	83.29 \pm 0.42	89.07 \pm 0.13	5.78 \blacktriangle	16.98 \pm 4.60	29.84 \pm 3.75	12.86 \blacktriangle
MIA	100.00 \pm 0.00	100.00 \pm 0.00	0.00-	98.23 \pm 0.38	99.61 \pm 0.09	1.38 \blacktriangle	85.57 \pm 2.32	90.10 \pm 0.69	4.53 \blacktriangle
RA	100.00 \pm 0.00	99.96 \pm 0.02	0.04 \blacktriangledown	99.51 \pm 0.21	98.16 \pm 0.79	1.35 \blacktriangledown	100.00 \pm 0.00	98.64 \pm 0.56	1.36 \blacktriangledown
TA	95.82 \pm 0.04	94.86 \pm 0.07	0.96 \blacktriangledown	95.33 \pm 0.19	94.16 \pm 0.08	1.17 \blacktriangledown	95.95 \pm 0.18	95.76 \pm 0.22	0.19 \blacktriangledown

Table A3. Performance of different unlearning methods under unwatermarked forget/retain sets (Original) and WATER4MU-induced watermarked forget/retrain sets on (CIFAR-10, SWIN TRANSFORMER) and (CIFAR-10, RESNET-50) for class-wise forgetting.

Metric	Retrain			GA			FT		
	Original	WATER4MU	Diff	Original	WATER4MU	Diff	Original	WATER4MU	Diff
Class-wise forgetting, SWIN TRANSFORMER, CIFAR-10									
UA	100.00 \pm 0.00	100.00 \pm 0.00	0.00-	45.96 \pm 0.67	55.43 \pm 0.50	9.47 \blacktriangle	94.89 \pm 1.56	99.80 \pm 0.17	4.91 \blacktriangle
MIA	100.00 \pm 0.00	100.00 \pm 0.00	0.00-	58.40 \pm 1.03	64.82 \pm 1.89	6.42 \blacktriangle	97.86 \pm 1.21	99.68 \pm 0.10	1.82 \blacktriangle
RA	100.00 \pm 0.01	99.71 \pm 0.07	0.29 \blacktriangledown	99.85 \pm 0.26	99.72 \pm 0.17	0.13 \blacktriangledown	95.01 \pm 1.26	93.45 \pm 0.92	1.56 \blacktriangledown
TA	85.63 \pm 2.10	85.34 \pm 1.27	0.29 \blacktriangledown	85.67 \pm 1.04	85.32 \pm 1.41	0.35 \blacktriangledown	80.58 \pm 2.16	78.32 \pm 1.67	2.26 \blacktriangledown
Class-wise forgetting, RESNET-50, CIFAR-10									
UA	100.00 \pm 0.00	100.00 \pm 0.00	0.00-	36.76 \pm 1.28	50.00 \pm 0.79	13.24 \blacktriangle	42.16 \pm 2.63	59.83 \pm 2.11	17.67 \blacktriangle
MIA	100.00 \pm 0.00	100.00 \pm 0.00	0.00-	59.60 \pm 0.65	77.66 \pm 1.03	18.06 \blacktriangle	58.35 \pm 1.53	67.75 \pm 1.93	9.40 \blacktriangle
RA	100.00 \pm 0.00	100.00 \pm 0.00	0.00-	99.84 \pm 0.08	99.53 \pm 0.19	0.31 \blacktriangledown	98.76 \pm 0.14	99.15 \pm 0.23	0.39 \blacktriangledown
TA	94.13 \pm 1.20	94.02 \pm 0.98	0.11 \blacktriangledown	93.67 \pm 0.72	93.12 \pm 1.57	0.55 \blacktriangledown	90.36 \pm 1.63	90.96 \pm 1.49	0.60 \blacktriangle

Table A4. Number of nude body parts detected by Nudenet on I2P dataset with threshold 0.6.

Method	Breast	Genitalia	Buttocks	Feet	Belly	Armpits	Total
SD v1.4	229	31	44	42	171	129	646
ESD	22	6	5	24	31	33	121
FMN	172	17	12	56	116	42	415
UCE	50	14	11	20	55	36	186
WATER4MU	29	15	5	10	29	21	109

the watermark message **m**. In our experiments, we set the message length L to 10 by default. We evaluate the decoding performance of HIDDEN used by WATER4MU. We find that its average BER is merely 2.78×10^{-8} compared to 1×10^{-8} using the standard HIDDEN w/o taking into account MU. This indicates that WATER4MU preserves the watermarking network’s encoding-decoding capabilities.

C.2. Additional class-wise forgetting results

As an expansion of Tab. 1, Tab. A2 presents the performance of class-wise forgetting with and without the integration of WATER4MU on the additional setups (CIFAR-100, RESNET-18) and (SVHN, RESNET-18). Also, Tab. A3 shows the performance of class-wise forgetting on the setups (CIFAR-10, SWIN TRANSFORMER) and (CIFAR-10, RESNET-50) to further validate the scalability of WATER4MU. Notably, the WATER4MU-integrated unlearning methods demonstrate enhanced unlearning performance across both datasets and models, as evidenced by improvements in UA and MIA metrics. This improvement effectively

balances model utility preservation, as reflected in RA and TA scores. Importantly, the gains in unlearning performance outweigh the losses in utility. These observations are consistent with the findings reported in Tab. 1.

C.3. Effect of Watermark Message Selection in WATER4MU.

In Fig. A2, we present the performance of the optimized watermark message, *i.e.*, selecting the watermark message most favorable for unlearning, as described in Sec. 5. As shown, using the optimized watermark message in WATER4MU further enhances unlearning effectiveness (UA and MIA) without causing any degradation in model utility (TA and RA). This improvement is particularly notable when compared to the use of random watermark messages in WATER4MU.

We also provide additional results on the impact of watermark message selection on Retrain. Extended from Fig. A2, Fig. A3 presents the performance of the optimized watermark message on the exact unlearning method, Retrain. As we can see, using the optimized watermark message in WATER4MU also enhances unlearning effectiveness of Retrain without causing any degradation in model utility, when compared to the use of random watermark message in WATER4MU.

C.4. Evaluation on image generation safety tasks.

We conduct experiments on the Inappropriate Image Prompts (I2P) dataset. Our evaluation focuses on the erasure of nudity. A total of 4703 images are generated with I2P prompts for

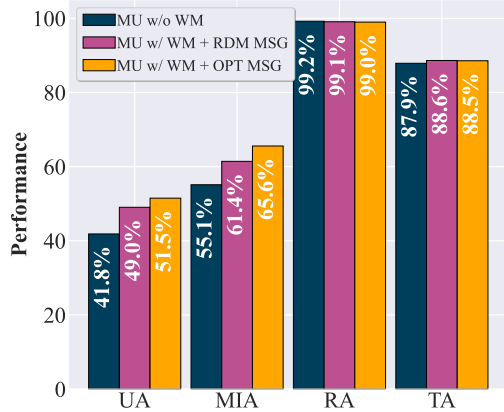


Figure A2. Performance of the optimized watermark message in WATER4MU. We choose GA as the unlearning method and compare the unlearning performance among MU without WATER4MU, MU with WATER4MU and MU with WATER4MU and optimized watermark message.

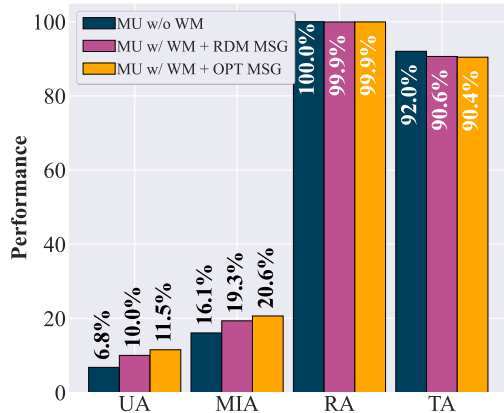


Figure A3. Performance of Retrain using the optimized watermark message in WATER4MU vs. baselines including MU without WATER4MU and MU with WATER4MU (but implemented using random watermark message).

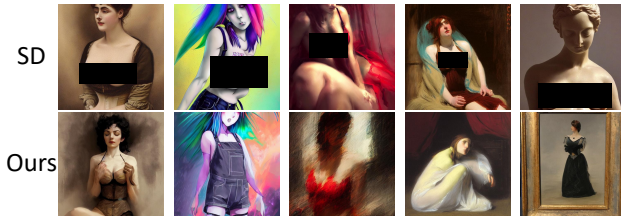


Figure A4. Qualitative results of nudity removing. All prompts originate from I2P dataset. The images in the top row are generated by SD, while the images in the bottom row are generated by MU with WATER4MU.

each model. Then, Nudenet is introduced to detect nude body parts in these images. As shown in Tab. A4, we present the number of detected nude body parts across six categories. WATER4MU achieves the best performance in preventing the generation of nude content, reducing the total instances

from 646 to 109. We provide more examples on the erasure of the nudity concept in Fig. A4.

D. Limitations

While WATER4MU demonstrates promising unlearning effectiveness, the introduction of the watermarking network and the computation of higher-order derivatives in the BLO process will both incur additional training overhead. Further work is needed to assess the scalability of WATER4MU to larger datasets and models, particularly in enhancing the efficiency of the bi-level optimization process used for watermarking design.